Comparison between UV Raman and circular dichroism detection of short alpha helices in bombolitin III.

ARTICLE *in* BIOCHEMISTRY · MARCH 2002

Impact Factor: 3.02 · Source: PubMed

3 AUTHORS, INCLUDING:

Abdil Özdemir
Sakarya University
31 PUBLICATIONS **265** CITATIONS
SEE PROFILE

Sanford A Asher
University of Pittsburgh
312 PUBLICATIONS **13,099** CITATIONS
SEE PROFILE

Comparison between UV Raman and Circular Dichroism Detection of Short α Helices in Bombolitin III†

Abdil Ozdemir, Igor K. Lednev, and Sanford A. Asher*

Department of Chemistry, University of Pittsburgh, Pittsburgh, Pennsylvania 15260

Received May 11, 2001; Revised Manuscript Received November 13, 2001

ABSTRACT: We have used UV resonance Raman (UVRR) and circular dichroism (CD) spectroscopies to examine the dilute solution-phase secondary structure of the 17 amino acid peptide Bombolitin III (BIII). Both UVRR and CD clearly observe the α-helix structure induced by the addition of trifluoroethanol (TFE) to BIII. In contrast, only UVRR is able to detect the single α-helical turn induced by increasing the pH of BIII from pH 1.8 to 6.4. This α-helical turn is formed because of a stabilizing salt bridge formed between Lys_2 and Asp_5. Further increases in the α-helix content occur as the pH is raised further. We compare the relative sensitivity of UVRR and CD to short α helices and find, as expected, that the CD cannot detect short α helices. This study demonstrates that UV Raman measurements can detect the formation of single α-helical turns which cannot be detected by CD measurements.

The field of proteomics would be significantly aided by the development of more incisive dilute solution methods to characterize protein structure, function, and dynamics. Although X-ray diffraction and multidimensional NMR[1] are considered to be the definitive structural techniques, these methods are limited in utility because of the extensive labor required to obtain protein structures. In addition, X-ray diffraction fails when crystals cannot be grown, and NMR fails when the molecules are too flexible or too large. Both X-ray and NMR also require relatively high quantities of often precious proteins and peptides. Thus, CD, IR absorption, and Raman spectroscopies are often used to obtain less complete, but still valuable, structural information, such as protein secondary structure, for example.

CD has a long and distinguished history as the primary technique for determining protein secondary structure in dilute solution (*1*). CD relies on the fact that the peptide α helix shows a large negative molar ellipticity, where the magnitude of the trough around 220 nm is monotonically related to the protein α-helical content (*2*). A number of approaches have been developed to quantitatively determine the α-helical content from the measured CD spectra. Many of these methods recognize that the magnitude of the CD molar ellipticity per residue decreases dramatically as the number of residues within an α helix decrease; thus, CD becomes less sensitive to α-helical content as the α-helical length decreases (*3*).

We are developing UV resonance Raman (UVRR) spectroscopy as a more powerful method for determining secondary structure. We have demonstrated that Raman spectra excited within the amide $\pi \rightarrow \pi^*$ transitions give rise to numerous intense spectral features which depend on the secondary structure (*4*). We recently developed a powerful spectral fitting methodology which calculates secondary structure by fitting the measured protein spectra to a series of basis spectra of the pure α-helix, random coil, and *β*-sheet conformations (*5*). We recently utilized this methodology to quantitatively examine the nanosecond dynamics of peptide and protein unfolding due to a T-jump (*6*, *7*). These studies were able to measure relaxation rates and activation barriers associated with α-helix-to-random coil conformational transitions.

In the work here, we directly compare the linearity of UV Raman versus CD in determining α-helical conformation. We demonstrate that by using UV Raman spectroscopy, we can easily detect the formation of a single α-helical turn (or *β* turn) in the peptide Bombolitin III (BIII) for a sample where CD finds negligible α-helix formation.

BIII is a heptadecapeptide which contains no aromatic amino acids and has the sequence Ile^1-Lys^2-Ile^3-Met^4-Asp^5-Ile^6-Leu^7-Ala^8-Lys^9-Leu^{10}-Gly^{11}-Lys^{12}-Val^{13}-Leu^{14}-Ala^{15}-His^{16}-Val^{17}-NH_2. Earlier, Holtz et al. (*8*) demonstrated using 206 nm excited UV Raman measurements that BIII has no α-helix content at low pH and suggested that a single α-helix turn forms at pH 7 because of the formation of a stabilizing salt bridge between the Lys_2 $-NH_3^+$ and the Asp_5 COO^-.

MATERIALS AND METHODS

The 17 amino acid peptide BIII was prepared (>95% purity) at the Pittsburgh Cancer Institute by using the solid-phase peptide synthesis method. Sodium hydroxide and hydrochloric acid obtained from Mallinckrodt and trifluoroethanol (TFE) obtained from Aldrich were used as received.

UV Raman excitation at 206.5 nm (∼1 mW) was obtained from a Coherent Inc. CW intracavity frequency-doubled krypton ion laser (*9*). The laser beam was focused into a 1 cm i.d. fused quartz cell containing 1 mL of a stirred 0.22

† This work was supported by NIH Grant GM30741.

* To whom correspondence should be addressed. E-mail: asher+@pitt.edu. Phone 412-624-8570. Fax: 412-624-0588.

[1] Abbreviations: NMR, nuclear magnetic resonance; IR, infrared; BIII, Bombolitin III; UV, ultraviolet; RR, resonance Raman; CD, circular dichroism; TFE, trifluoroethanol.

10.1021/bi010970e CCC: $22.00
Published on Web 01/15/2002

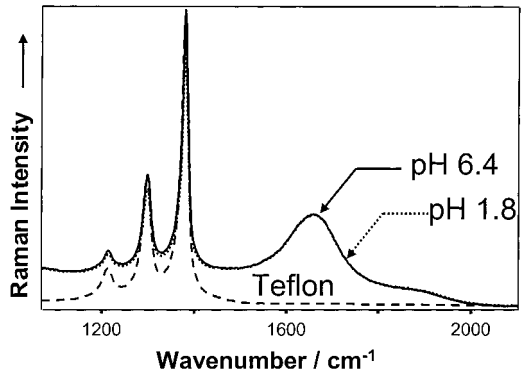

FIGURE 1: UVRR spectra of water (204 nm) at pH 6.4 and 1.8 measured in a 1 cm cuvette with a block of Teflon at the back. The Teflon acts as an external standard. The pH 6.4 and 1.8 UV Raman spectra of water completely overlap. Also shown is the spectrum of Teflon.

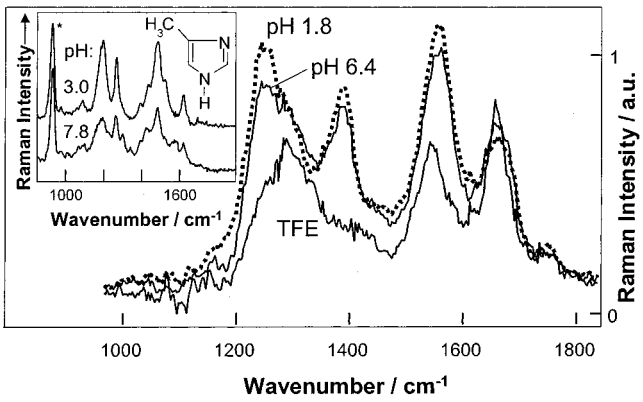

FIGURE 2: UVRR spectra of BIII at 206.5 nm excitation (0.22 mM) in water at pH 1.8 and 6.4 and at neutral pH in the presence of 22.5% (v/v) TFE. The spectra are normalized using the water Raman band as an internal standard. The inset shows the 206.5 nm UV Raman spectra of 4-methylimidazole (2.4 mM) at pH 3.0 and 7.8. The perchlorate Raman band (*) was used for normalizing the Raman spectra.

mM peptide solution. The Raman instrumentation used to collect, disperse, and detect the Raman scattered light has been described in detail elsewhere (*10*). Normally, we add an internal standard such as perchlorate to normalize the Raman spectra. However, because the BIII conformation is highly dependent on ionic strength, we could not use perchlorate and instead used the 1660 cm^{-1} bending water band as an internal standard to normalize the Raman spectra. As shown in Figure 1 the water bending band frequency, band shape, and intensity are independent of pH. The water spectra were subtracted from the BIII sample spectra after normalization.

We measured the UV absorption spectra by using a Perkin Elmer Lambda 9 absorption spectrometer. The CD spectra of BIII were measured in a 1 mm quartz cuvette at room temperature by using a Jasco 710 Spectropolarimeter.

RESULTS AND DISCUSSION

Figure 2 compares the 206 nm UV Raman spectra of BIII at pH 1.8, pH 6.4, and at neutral pH in 22.5% trifluoethanol (TFE), an α-helix promoter. At pH 1.8, BIII shows the Raman spectrum of a typical nonhelical peptide with the amide III band at 1248 cm^{-1}, the amide II band at 1557 cm^{-1}, the amide I band at 1664 cm^{-1}, and the $C_\alpha-H$ bending band

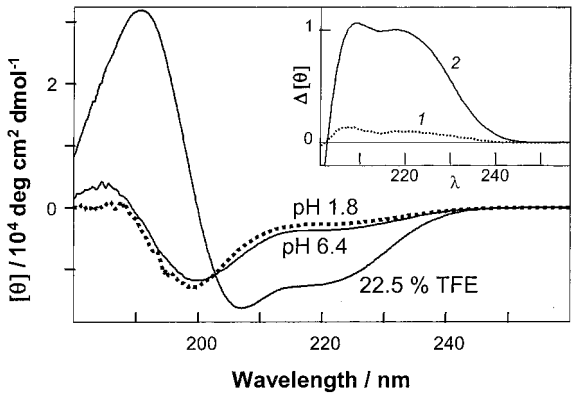

FIGURE 3: UV CD spectra of BIII obtained at the same conditions as those in Figure 2. The inset shows the difference CD spectra between those measured at (1) pH 1.8 and 6.4 and (2) pH 1.8 and neutral pH in the presence of 22.5% TFE.

Table 1: UVRR-Determined pH Dependence of BIII Secondary Structure

pH	α helix (%)	random coil (%)	β sheet (%)
1.8	0	63	37
4.6[a]	13	47	40
6.4	17.5	44	40.5
8.0[a]	25	39	36
9.3[a]	48	21	31
10.3[a]	60	21	19
TFE[b]	69	34	−3

[a] Data from ref *8*. [b] For 22.5% (v/v) TFE in water.

at 1390 cm^{-1}. The Figure 2 inset shows the UV Raman spectra of 4-methylimidazole at pH 3.0 and 7.8. The pH 3.0 spectrum shows a strong 1200 cm^{-1} ring-stretching mode that would be contributed by the protonated BIII histidine ring, as discussed in the following paragraphs.

Addition of TFE converts the spectrum to that of a dominantly α-helical peptide; the amide III band shifts to ∼1300 cm^{-1}, and the $C_\alpha-H$ bending vibration at 1390 cm^{-1} disappears. The Figure 3 CD spectra of BIII confirm this TFE-induced structural change; the pH 1.8 sample shows the CD spectrum of a non-α-helical peptide, while the sample containing TFE shows an α-helical CD spectrum with a trough at ∼220 nm.

We calculated the α-helical content of the low pH and TFE BIII samples from the UV Raman spectra by using the methodology of Chi et al. (*5*) and their basis spectra. The only difference was that we did not utilize the >1600 cm^{-1} part of the spectrum, which contains the amide I band, because this band only shows modest changes and because this region can be confounded by the overlapping water bending vibration. We calculate (Table 1) that the pH 1.8 BIII has zero α-helix, 63% random coil, and 37% β-sheet content. In contrast, the TFE BIII is 69% α-helix and 34% random coil.

A single α-helix turn should give rise to α-helical amide II and III Raman bands because each amide bond appears to independently contribute its amide II and III bands to the Raman spectrum (*11*). In contrast, the amide I vibration involves a vibrational mode delocalized over numerous amide bonds. For example, the Hochstrasser group (*12*) IR absorption measurements indicate that the amide I vibration involves coupling of 3−4 peptide bonds, because the large amide I dipole moment interacts through transition dipole

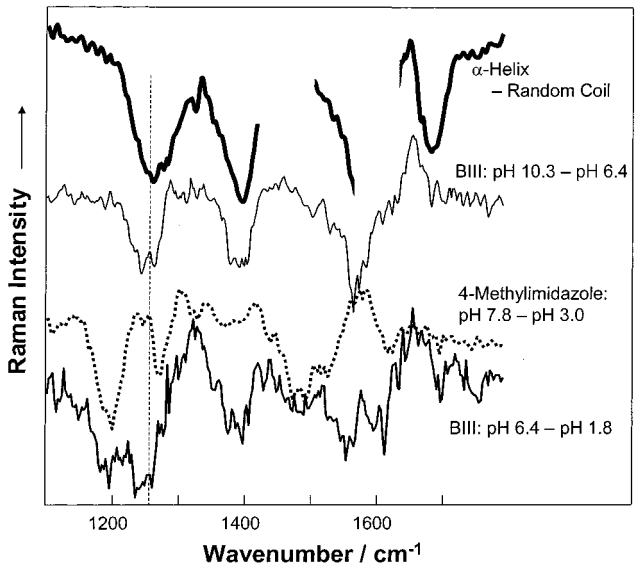

FIGURE 4: Raman spectroscopic signatures of formation of α helices. Shown are BIII Raman difference spectra between pH 6.4−1.8 and pH 10.3−6.4 and 4-methylimidazole difference spectrum between pH 7.8−3.0. Also shown is the Raman difference spectrum between the "average" pure α-helix and unordered secondary structure basis spectra (*5*).

coupling. This presumably is the origin of the α-helix length dependence of the amide I IR absorption spectra (*13*, *14*).

A number of methods have previously been used to estimate α-helix content from CD spectra. We utilized the K2D, Dichro, and the Lifson-Roig 222 nm helix coil model within an easily used program available at http://pbil.ibcp.fr/DICROPROT to calculate the BIII secondary structure. These methods gave between 0% and 13% α helix at pH 1.8, with the best spectral fit suggesting 5% α helix. For TFE the various methods gave values between 23% and 52% α helix.

At pH 6.4, the BIII UV Raman spectrum signals a significant change in secondary structure as compared to pH 1.8, while the CD shows little change (Figures 2 and 3). As discussed below, if the CD spectra change linearly with increasing α-helical content, the observed small CD changes would correlate with only a 3% α-helical content increase. A pH increase from 1.8 to 6.4 causes the Raman intensities of the 1248 cm^{-1} amide III, the 1557 cm^{-1} amide II, the 1664 cm^{-1} amide I, and the 1390 cm^{-1} C_α−H bending band to decrease, while a small intensity increase occurs at ∼1300 cm^{-1}, the location of the α-helix amide III band. As evident for the TFE BIII sample, the Raman cross sections of the amide II and III bands are more than 2-fold smaller in α-helical peptides as compared to that in random coil and β-sheet peptides. We calculate that the pH 6.4 BIII sample contains 18% α helix, close to the 22% α-helical content calculated by Holtz et al. (*8*). As shown in Figure 4, the UV Raman difference spectrum between pH 6.4 and 1.8 is identical to that between pH 10 and 6.4 except for the additional 1748 cm^{-1} carboxyl deprotonation trough and the 1200 cm^{-1} histidine deprotonation trough in the pH 6.4−1.8 difference spectra (*15*). Both pH difference spectra are essentially identical to the difference spectrum between a pure α helix and a pure random coil basis spectra (Figure 4). Thus, these data indicate that BIII forms a single α-helical turn at pH 6.4, as previously noted by Holtz et al. (*8*).

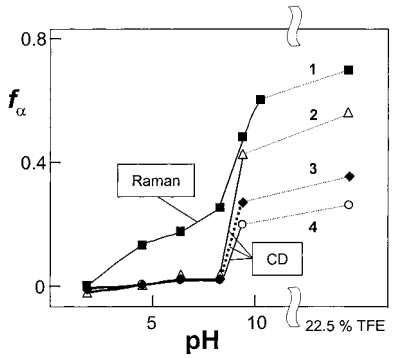

FIGURE 5: Fractional helicity of BIII estimated from Raman and CD spectra. The CD estimates utilized eq 1 and 222 nm molar ellipticities for random coil, $[\theta]_R = -3000$ (deg cm^2)/dmol. We also utilized α helix $[\theta]_\alpha$ values of (2) −20 000, (3) −30 000, and (4) −40 000 (deg cm^2)/dmol, which were assumed to be independent of α-helix length. Data are also shown for BIII at neutral pH in the presence of 22.5% TFE.

It is surprising that a single α-helical turn would form because of the Lys_2 and Asp_5 ion pair, since α-helical formation is entropically costly and only ∼1 compensating α-helix hydrogen bond would be formed. Formation of this helical turn may be due to the fact that the Met and Ile intervening residues have strong propensities for α-helix formation, and the size of these residues may prevent formation of type II β turns. We cannot, however, rule out the formation of a type I β turn because we have not as yet characterized its Raman spectrum. Some of the residues of a type I β turn have ϕ, ψ angles not far from that of an α helix. However, it is unlikely that a β turn occurs because other residues have very different ϕ, ψ angles, which should give detectable shifts in the Raman difference spectra (*16*).

In contrast to the Raman spectra, the pH 6.4 CD spectrum is essentially identical to that at pH 1.8. This clearly indicates a lack of sensitivity for CD to this single α-helical turn. The CD modeling methodologies are clearly able to detect the major increase in the α-helix content due to the presence of TFE but find α-helical content changes between pH 1.8 and 6.4 of at most ∼3%.

Figure 5 compares the fractional helicity estimated from Raman and CD spectra, where the CD helicity, f_α, was estimated by

$$f_\alpha = \frac{[\theta] - [\theta]_R}{[\theta]_\alpha - [\theta]_R} \quad (1)$$

Thus, CD detects little α-helix formation until pH > 8. This lack of CD sensitivity to a single α-helical turn is expected, because, for example, the 222 nm molar ellipticity per residue for an α helix is predicted to be zero for a single helix

$$[\theta]_n = [\theta]_\infty(1 - k/n) \quad (2)$$

where $[\theta]_n$ is the value of the molar ellipticity per residue for a residue of n amino acid residues, while $[\theta]_\infty$ is the value of the molar ellipticity per residue for an infinitely long helix ($[\theta]_\infty = 40\,000$ deg cm^2/dmol) and $k = 4.3$, an empirically determined constant. Thus, $[\theta]_n \sim 0$ for a single helical turn. Figure 6 shows the calculated helix length dependence of $[\theta]_n$ and the values which would occur for the different BIII pH values.

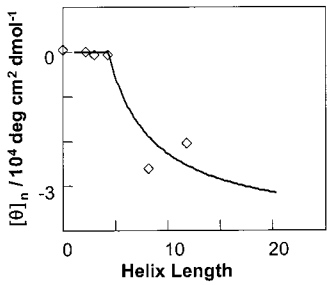

FIGURE 6: Helix-length dependence of the molar ellipticity per helical residue, $[\theta]_n$. The helix length was determined from Raman measurements at different pH values (see Table 1). The solid curve is obtained using eq 2 with $[\theta]_\infty = -40\,000$ (deg cm^2)/dmol and $k = 4.3$ (*3*, *17*, *18*).

The helical molar ellipticity values were estimated from pH and TFE-dependent CD data using

$$[\theta]_n = ([\theta]_{222} - [\theta]_R)(N/n) + [\theta]_R(1 - k/n) \qquad (3)$$

where $[\theta]_{222}$ is the measured 222 nm molar ellipticity, $[\theta]_R$ is the low pH fully random coil 222 nm molar ellipticity, and $N = 17$ is the total number of amino acid residues in BIII. Equation 3 takes into account that the k α-helical residues that do not contribute to the helical CD spectrum must contribute to the random coil CD spectrum. The latter is based on the fact that the CD spectra of fully unordered BIII (pH 1.8) and that containing one helical turn (pH 6.4) are close to each other (Figure 3). Thus, as the length of an α-helix increases, the magnitude of $[\theta]_n$ will rapidly increase and CD should become more sensitive to the formation of α-helical residues.

The CD phenomenon results from interpeptide bond coupling of magnetic and electric dipole transition moments of coupled α-helix peptide bond electronic transitions. This coupling should increase with the length of the helix. Thus, a minimum CD signature should occur for a single turn. In contrast, the Raman effect appears to be more linear, where each peptide bond independently contributes to the Raman intensity. The spectrum contributed by each peptide bond depends on its Ramachandran ϕ and ψ angles. However, some nonlinearity may occur in the Raman spectra due to hypochromicity. It is well-known that the formation of α helices results in hypochromism. Because the Raman cross section depends on the square of the molar absorptivity, the magnitude of the α-helical contribution to the Raman spectrum could decrease for longer α-helical lengths. However, this should have only a minor, if any effect, for very short helices.

Bombolitins can show aggregation phenomena which promote α-helix formation. It is unlikely that our results derive from a pH-induced aggregation, which leads to α-helix formation. This equilibrium would result in a low concentration of long helices which would result in similar CD and Raman sensitivities.

In conclusion, this study demonstrates that UV Raman measurements can detect the formation of single α-helical turns, which cannot be detected by CD measurements.

ACKNOWLEDGMENT

We gratefully acknowledge Dr. Robert W. Woody for valuable discussions, Alex Mikhonin for technical assistance, and Mary Boyden for providing the Raman spectra of methylimidazole.

REFERENCES

1. (1996) *Circular Dichroism and the Conformational Analysis of Biomolecules* (Fasman, G. D., Ed.), Plenum Press, New York.
2. Venyaminov, S. Yu., and Yang, J. T. (1996) in *Circular Dichroism and the Conformational Analysis of Biomolecules* (Fasman, G. D., Ed.), Chapter 3, pp 69−108, Plenum Press, New York.
3. Woody, R. W. (1996) in *Circular Dichroism and the Conformational Analysis of Biomolecules* (Fasman, G. D., Ed.), Chapter 2, pp 25−68, Plenum Press, New York.
4. Song, S., and Asher, S. A. (1989) *J. Am. Chem. Soc. 111*, 4295−4305.
5. Chi, Z., Chen, X. G., Holtz, J. S. W., and Asher, S. A. (1998) *Biochemistry 37*, 2854−2864.
6. Lednev, I. K., Karnoup, A. S., Sparrow, M. C., and Asher, S. A. (2001) *J. Am. Chem. Soc. 123*, 2388−2392.
7. Lednev, I. K., Karnoup, A. S., Sparrow, M. C., and Asher, S. A. (1999) *J. Am. Chem. Soc. 121*, 8074−8086.
8. Holtz, J. S. W., Holtz, J. H., Chi, Z., and Asher, S. A. (1999) *Biophys. J. 76*, 3227−3234.
9. Holtz, J. S. W., Bormett, R. W., Chi, Z., Cho, N., Chen, X. G., Pajcini, V., Asher, S. A., Arrogoni, M., Qwen, P., and Spinelli, L. (1996) *Appl. Spectrosc. 50*, 1459−1468.
10. Asher, S. A. (1993) *Anal. Chem. 59−66A*, 201−210A.
11. Mix, G., Schweitzer-Stenner, R., and Asher, S. A. (2000) *J. Am. Chem. Soc. 122*, 9028−9029.
12. Hamm, P., Lim, M., and Hochstrasser, R. M. (1998) *J. Phys. Chem. 102B*, 6123−6138.
13. Nevskaya, N. A., Chirgadze, and Yu, N. (1976) *Biopolymers 15*, 637−648.
14. Graff, D. K., Pastrana-Rios, B., Venyaminov, S. Yu., and Prendergast, F. G. (1997) *J. Am. Chem. Soc. 122*, 11282−11294.
15. Austin, J. C., Jordan, T., and Spiro, T. G. (1993) in *Biomolecular Spectroscopy* (Clark, R. J. H., and Hester, R. E., Eds.) Part A., Chapter 2, pp 55−127, John Wiley and Sons Ltd., New York.
16. Krimm, S., and Bandekar, J. (1980) *Biopolymers 19*, 1−29.
17. Gans, P. J., Lyu, P. C., Manning, M. C., Woody, R. W., and Kallenbach, N. R. (1991) *Biopolymers 31*, 1605−1614.
18. Chen, Y.-H., Yang, J. T., and Chau, K. H. (1974) *Biochemistry 13*, 3350−3359.

BI010970E